

NEURONAL CODING OF SPATIAL VISUAL INFORMATION

Ph.D. Thesis

Gabriella Eördegh

**Department of Physiology, Faculty of Medicine, University of Szeged,
Szeged**

2007

Table of contents

Table of contents	2
List of publications related to the subject of the thesis	3
1. Introduction	4
<i>1.1. Morphological connections within the extrageniculate pathways</i>	<i>4</i>
<i>1.2. Physiological properties of the extrageniculate visual structures</i>	<i>6</i>
<i>1.3. Coding of visual, auditory and multisensory spatial information</i>	<i>7</i>
<i>1.4. Cortico-thalamic and thalamo-cortical flow of information</i>	<i>9</i>
2. Aims of the study	11
3. Materials and methods	12
<i>3.1. Animal preparation and surgery</i>	<i>12</i>
<i>3.2. Recording</i>	<i>13</i>
<i>3.3. Stimulation and data analysis to compare the internal organisation of the visual receptive fields in the AEV and the LM-Sg</i>	<i>13</i>
<i>3.4. Stimulation and data analysis to investigate the extent of multisensory receptive fields and the coding of multisensory information in the AEV</i>	<i>14</i>
<i>3.5. Calculation of the visual response onset latencies</i>	<i>16</i>
4. Results	17
<i>4.1 Internal organisation of the visual receptive fields in the AEV and the LM-Sg</i>	<i>17</i>
<i>4.2. Extent of visual, auditory and bimodal receptive fields of the AEV neurons</i>	<i>18</i>
<i>4.3. Coding of multisensory information in the AEV</i>	<i>19</i>
<i>4.4. Visual response onset latencies of the AEV and the LM-Sg neurons</i>	<i>21</i>
5. Discussion	23
<i>5.1. Comparison of the internal organisation of visual receptive fields in the AEV and the LM-Sg</i>	<i>23</i>
<i>5.2. Objective estimation of the extent of visual and bimodal receptive fields in the AEV</i>	<i>23</i>
<i>5.3. Coding of multisensory information in the AEV</i>	<i>24</i>
<i>5.4. The relay function of the LM-Sg</i>	<i>26</i>
6. Conclusions	28
7. Summary	29
8. Acknowledgments	32
9. References	33
10. Figures and figure captions	41

List of publications related to the subject of the thesis

I. Benedek G, Norita M, Hoshino K, Katoh YY, **Eördegh G**, Nagy A (2003) Extrageniculate visual pathways in the feline brain. In: Dumitrascu DL (editor) Psychosomatic Medicine; Recent progress and current trends. "Iuliu Hatieganu" University Publishing House, Cluj, Romania, pp 33-40. ISBN: 973-8385-62-8

II. Nagy A, **Eördegh G**, Benedek G (2003) Extents of visual auditory and bimodal receptive fields of single neurons in the feline visual associative cortex. Acta Phys Hung 90:305-312

III. Hoshino K, Nagy A, **Eördegh G**, Benedek G, Norita M (2004) Two types of neuron are found within the PPT, a small percentage of which project to both the LM-SG and SC. Exp Brain Res 155:421-426
Impact factor: 2.118

IV. Benedek G, **Eördegh G**, Chadaide Z, Nagy A (2004) Distributed population coding of multisensory spatial information in the associative cortex. Eur J Neurosci 29:525-529
Impact factor: 3.949

V. **Eördegh G**, Nagy A, Berényi A, Benedek G (2005) Processing of spatial visual information along the pathway between the suprageniculate nucleus and the anterior ectosylvian cortex. Brain Res Bull 67:281-289
Impact factor: 2.481

1. Introduction

The existence of separate geniculate and extrageniculate visual systems in the feline brain has been proved in both morphological and physiological studies. Besides the dorsal lateral geniculate nucleus (LGNd), several subcortical structures have been found that receive afferents directly from the retina (Rosenquist, 1985). One of them is the superior colliculus (SC), whose neurons provide the origin for the tectal extrastriatal pathways that has attracted most research interest in the course of the past twenty-five years. The investigations of the extrageniculate visual system started in 1969 when Loe and Benevento (1969) described a multimodal sensory area over the anterior part of the cat brain. The story of the extrageniculate visual pathways continued in the early 1980s when Otto Creutzfeldt and Lennart Mucke attempted to record visual neurons in the claustrum via stereotaxic targeting. They were repeatedly able to record visually highly active neurons, but on histological control these turned out to be located outside the border of the caudal portion of the claustrum. This serendipitous finding yielded to the discovery of a novel visual area along the anterior ectosylvian sulcus (AES) (Mucke et al., 1982) and focused the investigations to clarify its physiological properties and its afferent and efferent connections. It should be noted that Olson and Graybiel (1983), who had similarly searched for visual activity in the claustrum, simultaneously detected the existence of the anterior ectosylvian visual area (AEV). This visual region extend throughout almost the whole length of the AES, including its rostral gyral cortical region; this was called the insular visual area (IVA) (Benedek et al., 1986; Hicks et al., 1988a; b; Norita et al., 1991), a name that was later found to be not totally appropriate (Reinoso-Suares and Roda, 1985).

1.1. Morphological connections within the extrageniculate pathways

Morphological experiments have confirmed that the SC is a main source of visual information toward the AEV (Harting et al., 1992). The AEV now seems to be the only cortical visual area that visual afferentation entirely bypasses the lateral geniculate complex and the primary visual cortex (A17) (Rosenquist, 1985), thus receives clearly extrageniculo-extrastriatal visual information. The excitatory Y inputs from the retinal ganglion cells dominate the responses of neurons in the intermediate and deep layers of the SC and AEV (Wang et al., 1998; 2001). The SC sends hard afferentation to the AES cortex

via the extrageniculate thalamus. The AEV receives thalamic afferents mainly from the lateralis medialis-suprageniculate nuclear complex (LM-Sg) of the posterior thalamus, and a smaller proportion of the afferentation coming from the medial part of the nucleus lateralis posterior (LPm) (Norita et al., 1986). The LM-Sg complex has evaded thorough morphological and physiological analysis because of problems with the definition of its borders. Acetylcholinesterase staining provided a possibility to circumscribe and locate this thalamic area exactly (Hardy et al., 1976). Anatomical tracing experiments proved that there is a noteworthy convergence of inputs from a wide anteroposterior and mediolateral aspect of the intermediate and deep layers of the SC to the neurons in the LM-Sg (Hicks et al., 1986; Katoh et al., 1995; Katoh and Benedek, 1995). The main source of the cortical afferentation to the AEV is the posterior-medial division of the lateral suprasylvian (PMLS) area (Miceli et al., 1985; Norita et al., 1986). The predominant targets of efferentation of the visual neurons along the AES are the LM-Sg. Thus the cortico-thalamic, AEV-LM-Sg route is also highly active. The important and opened question concerning the LM-Sg-AEV pathways is the primarily direction of the information flow. Then, as regards the direction of the information flow, are the cortico-thalamic and thalamo-cortical routes equally active during visual information processing? The AEV send further afferentation to the intermediate and deep layers of the SC, to the PMLS area, to the frontal eye fields, to the amygdala and other cortical and subcortical structures, out of the lateral geniculate complex and the A17 region (Norita et al., 1986; Harting et al., 1992). The LM-Sg complex of the thalamus receives efferents from both the fastigial nuclei of the cerebellum (Katoh et al., 2000; Katoh and Benedek, 2003) and the pedunculopontine tegmental nucleus (PPT) (Hoshino et al., 2000; 2004). The functional importance of the LM-Sg and the SC-LM-Sg-AEV axe is that it seems to provide the visual and multisensory information toward the basal ganglia, i.e. to the caudate nucleus (CN) the substantia nigra (SN) and the subthalamic nucleus (Harting et al., 2001 a; b; Comoli et al., 2003; Nagy et al., 2003; 2005a; b; Jiang et al., 2003). Thus the SC-LM-Sg-AEV axis seems to be critical for the sensory-motor integration function of the CN and the SN concerning the sensory feedback of motor actions controlled by the basal ganglia. Figure 1 shows the most relevant morphological connection within the extrageniculate visual system.

1.2. Physiological properties of the extrageniculate visual structures

Early observations demonstrated that the AEV neurons possess particular visual receptive field properties (Mucke et al., 1982; Benedek et al., 1988). All the experiments were performed on anesthetized, immobilized, artificially respirated cats with extracellular single unit recordings. Very similar receptive field properties have been found in neurons in the IVA (Benedek and Hicks, 1988; Hicks et al., 1988a; b), in the intermediate and deep layers of the SC (Stein and Meredith, 1993), in the LM-Sg (Benedek et al., 1997), in the CN (Nagy et al., 2003b) and the SN (Nagy et al., 2005a). Hence, we can summarize the visual receptive field properties, irrespectively of the region in question. A striking physiological characteristic of these neurons is the overwhelming sensitivity of the neurons to movement in their receptive field. The neurons are not or very poor sensitive to static visual stimulation and flash of the light stimuli. Colour and shape sensitivity was also not described. The neurons are primarily sensitive to very small stimuli moving very rapidly in a specific direction in their huge receptive field (Benedek et al., 1988; 1997; Hicks et al., 1988b). A substantial proportion (approximately 20%) of the AEV neurons responds optimally to extremely high velocities, higher than 1000 degree/second. Most of the neurons are highly direction-selective. Several neurons have also been found that failed to show end-inhibition properties and ones that did not prefer extremely high stimulus velocities, but clearly no neuron was observed which exhibited the velocity properties demonstrated in the striate area (Benedek and Hicks, 1988). While the neurons were not responsive or elicited only weak responses to static visual stimulation, it was not easy to draw the exact borders of their receptive fields. The receptive field mappings that were the results of subjective observations where visual stimuli were generated with hand-held lamps and projectors and the neuronal responses were heart described large but well-localized receptive fields and a limited retinotopic organisation in the AEV (Olson and Graybiel, 1987; Scannel et al., 1996). Despite of these findings, earlier studies of our laboratory suggest extremely large receptive fields and no signs of retinotopical organization within the whole tectal visual system. The visual receptive fields consistently include the area centralis and practically equal with the visual field of the investigated eye (Mucke et al., 1982; Benedek et al., 1988; Hicks et al., 1988b; Nagy et al., 2003; 2005a). To solve this discrepancy we introduced a quasi-objective, computer-controlled method to investigate the extent of visual and multisensory receptive fields of the AEV neurons.

An interesting aspect of the tecto-thalamo-cortical system is its sensitivity to various sensory modalities. The tectal originated extrageniculate system seems to be multisensory conveying also auditory and somatosensory information. The multimodal character of the intermediate and deep layers of the SC has been extensively studied (Meredith and Stein, 1986; Meredith et al., 1992). It emerged that there is a heavy representation of auditory and somatosensory modalities in both the LM-Sg, the cortex along the banks of the AES (Hicks et al., 1988a; Jiang et al., 1994; Benedek et al., 1997) and the basal ganglia (Nagy et al., 2005b). The extents of the auditory receptive fields in the AEV were extremely large covering 360° of azimuth of the horizontal plane (Middlebrooks et al., 1994; 1998; 2002). They also observed that neurons in the nontopographical cortex were not organized in a topographical order concerning their optimal spatial location of sound sources. The somatosensory receptive fields are also extremely large. Somatosensory neurons can be activated by stimulation of the whole body surface of the animal. No sign of somatotopical organization was detected. A high number of multisensory (bimodal and even trimodal) cells have also been found (Benedek et al., 1996; 1997; Nagy et al., 2005b). Such brain structures that process multisensory information and contain multisensory single cells have the possibility to integrate visual, auditory and somatosensory information. Multisensory integrations, i.e. multisensory response enhancement and depression were earlier described in the superior colliculus (SC) (Hicks et al., 1988a; Meredith and Stein, 1986, Wallace et al., 1998) but not widely investigated in another structures along the SC originated visual system. The corresponding behavioural consequence of these cross-modal interactions is a substantial increase in the probability of a correct response to a sensory event (Stein et al., 1989) and a substantial decrease in reaction time (Goldring et al., 1996; Taylor et al., 1999). Despite the large number of multisensory neurons found in the AEV we have hitherto no information concerning the multisensory integration ability of the visual associative cortex.

1.3. Coding of visual, auditory and multisensory spatial information

The traditional topographical code, i.e. retinotopical and somatotopical organization assumed that single neurons are selective for particular stimulus locations and the stimulus-source locations are coded by the cortical location of a small population of maximally activated neurons (Tusa et al., 1978; Middlebrooks et al., 1998). The LGNd and the A17

display a strict retinotopic organization of neurons with rather small, well-localized receptive fields (Hubel and Wiesel, 1961; 1962; Sanderson, 1971).

In contrast the neurons of cortical and subcortical structures of the SC originated pathways have a receptive field organization and structure rather different from those of the A17 and the LGNd. The receptive fields are large, consistently cover the area centralis. Thus in contrast with the impressive retinotopy in the geniculostriatal pathway (Tusa et al., 1978) we found the complete absence of retinotopic organization (Mucke et al., 1982; Benedek et al., 1988; Hicks et al., 1988b; Nagy et al., 2003; 2005a) in the tectal extrageniculate visual system. The absence of traditional topographic coding and retinotopical organization in the AES cortex gave rise to the idea that there could be another type of spatial coding in this system. Neurophysiological studies on the optic tectum in birds demonstrated that single neurons have the ability to provide information on the site of the stimulus source within their large receptive field (Knudsen, 1982). Thus they can serve as panoramic localizers. Such panoramic localizers were later described in invertebrates (Bialek et al., 1991; Nalbach et al., 1993) and in the mammalian SC (Palmer and King, 1982; Jay and Sparks, 1984; Middlebrooks and Knudsen, 1984; King and Hutchings, 1987). These panoramic localizer neurons can code information from sound source (Middlebrooks, 1998), somatosensory stimuli (Lewis, 1999) and the direction or amplitude of saccadic eye movements (Lee et al., 1988). The accurate stimulus source localization derives from information that is distributed a large population of such panoramic neurons. This distributed population coding seems to be similar accurate and can carry the same amount of information about the stimulus properties as the classical topographical code (Bialek, 1991; Lewis, 1999). Not many data have accumulated however, concerning the existence of such a population code based on panoramic localizers in the mammalian cortex. Earlier observations provided evidence of the panoramic stimulus-localizing ability of neurons and a distributed population code of auditory information in the nontopographic auditory cortex along the AES of the feline brain. (Middlebrooks et al., 1994; 1998; 2002; Brugge et al., 2001). Benedek et al. (2000) described in a preliminary report, that visual neurons, similarly to the auditory ones (Furukawa et al., 2000; Middlebrooks et al., 1994), reveal a spatial localization function, at least in the central part of their large visual receptive field (Benedek et al., 2000). Nonetheless, the internal organization of the whole receptive fields and the stimulus source localizing of the visual and multisensory AEV and LM-Sg neurons waiting further investigation. The questions remain open whether the visual and multisensory AEV and

LM-Sg neurons similarly to the auditory neurons are panoramic localizers and whether there is a distributed population code of multisensory spatial information in the AES cortex and the LM-Sg. Special attention has been paid to bimodal cells that react to both visual and auditory modalities in order to determine whether the bimodal information and the cross-modal interactions may improve the localizing ability of a single AEV neuron.

1.4. Cortico-thalamic and thalamo-cortical flow of information

The function of the thalamus in the mammalian brain is based on the existence of two types of relays (Sherman and Guillery, 1998; 2002; Guillery et al., 2002; Guillery and Sherman, 2002). Thalamic first-order relays receive their driving afferents from ascending pathways and transmit messages to the cortex that the cortex has not received before. Higher-order relays bring driver messages to the thalamus from the cortex for transmission from one cortical area to another. This ambiguity stresses the importance of the cortico-thalamic and the thalamo-cortical pathways. There are thalamic nuclei that receive driving from both the cortex and lower centres. The best-known such nuclei are the pulvinar and the lateralis posterior nuclei, which receive driving afferents from the visual cortex, and there is an additional tectal input to them (Casanova et al., 2001; Merabet et al., 1998). Similarly, Sommer and Wurtz (2004) described that the medial dorsal nucleus of the thalamus that innervates the frontal eye field receives drive from both the cortex and the intermediate and deep layers of the SC, but its main drive arrives from the tectal region. These thalamic nuclei process messages that have already reached the cortex and been processed in at least one cortical area, and at the same time they serve the role of first-order relays receiving signals from the ascending pathways. Since the LM-Sg receives heavy afferentation both from the intermediate and deep layers of the SC (Katoh and Benedek, 1995) and from the visual associative cortex along the AES (Hicks et al., 1986) a similar ambiguity seems to characterize the role of the LM-Sg of the thalamus and its connections with the cortex along the AES. In contrast with the LGNd that relays the retinal input towards the primary visual cortex without causing any fundamental modification in the size of the receptive fields, the visual receptive fields in the LM-Sg are rather dissimilar to those of the neurons of the intermediate and deep layers of the SC. The receptive fields of the LM-Sg neurons uniformly cover the whole extent of the visual field of the stimulated eye (Benedek et al., 1997; Hicks et al., 1986). These receptive field properties can appear

for two reasons. The strong convergence of the collicular fibres on the LM-Sg (Kato and Benedek, 1995) could be responsible for the representation of the whole visual field. The LM-Sg might mediate this information to the cortex, and thus the similarly huge receptive fields of the neurons along the AES (Benedek et al., 1988; Hichs et al., 1988; Mucke et al., 1982) could be a consequence of the thalamic relaying of this convergence. On the other hand, the activity of the pathway between the visual associative cortex (AEV) and the LM-Sg (Hicks et al., 1986; Updyke, 1981) could also result in the large receptive fields of LM-Sg neurons. This raises at least two important questions concerning the visual information processing and flow between the AES cortex and the LM-Sg: Is the internal organization of the large receptive fields of the LM-Sg units similar to or different from that of the AEV (Benedek et al., 2000)? Then, as regards the direction of the information flow, are the cortico-thalamic and thalamo-cortical routes equally active during visual information processing?

2. Aims of the study

The aims of our experiments were to investigate an alternative coding mechanism of visual and multisensory information in the visual associative cortex along the AES and in its thalamic projection zone, the LM-Sg nuclei complex and to determine the direction of information flow between the AEV and the LM-Sg of the mammalian brain. Our exact aims were:

1. To investigate the spatial coding abilities of the LM-Sg and the AEV neurons and to compare the internal organization of the visual receptive fields of the LM-Sg and the AEV single-cells.
2. To calculate the visual response onset latencies of the AEV and the LM-Sg neurons in order to demonstrate the direction of visual information flow between the AES cortex and the LM-Sg.
3. To investigate the relay function of the LM-Sg, whether the LM-Sg is a first order or a higher order thalamic relay nucleus of the visual information.
4. To investigate whether the visual and multisensory AEV neurons are panoramic localizers.
5. To investigate whether there is a distributed population code of visual and multisensory information in the AEV so as to acquire a better understanding of the multimodal representation of the environment in the mammalian brain.
6. To compare the visual, auditory and multisensory stimulus-source localizing of the single multisensory AEV neurons.
7. To provide evidence on the multisensory integration in the single AEV cells.

3. Materials and methods

3.1. Animal preparation and surgery

This study was performed on 17 adult cats of either sex weighting between 2.8 and 3.5 kg. All procedures were carried out to minimize the number of the animals and followed the European Communities Council Directive of 24 November 1986 (S6 609 EEC) and the National Institutes of Health guidelines for the care and use of animals for experimental procedures. The experimental protocol was accepted by the Ethical Committee for Animal Research of Albert Szent-Györgyi Medical and Pharmaceutical Center at the University of Szeged. The cats were initially anesthetized with ketamine hydrochloride (30 mg/kg i.m.). The trachea and the femoral vein were cannulated and the animals were placed in a stereotaxic headholder. The animal's head was fixed to a vertical metal bar with the aid of acrylate and the ear-bars were removed. Wound edges were treated generously with procaine hydrochloride (1%). The anaesthesia was continued with halothane (1.6% during surgery and 0.8% during recordings). The depth of anaesthesia was monitored by continuous reading of end-tidal halothane values and by repeated checks of the electroencephalogram (EEG) and electrocardiogram. There was continuous high-amplitude, low-frequency EEG activity and we checked repeatedly whether any interventions or a forceful pressing of the forepaws could induce desynchronization. The MAC values calculated from the end-tidal halothane readings always lay in the range given by Villeneuve and Casanova (2003). The animals were immobilized with gallamine triethiodide (Flaxedyl, 20 mg/kg i.v.). A liquid containing gallamine (8 mg/kg/h), glucose (10 mg/kg/h) and dextran (50 mg/kg/h) in Ringer's solution was infused at a rate of 3 ml/h. The end-tidal CO₂ level and the rectal temperature were monitored continuously and kept approximately constant, at 3.8-4.2% and 37-38 °C, respectively. The skull was opened with a dental drill to allow a vertical approach to the appropriate brain structures. The dura mater was removed and the cortical surface was covered with a 4% solution of 38 °C agar dissolved in Ringer solution. The eye contralateral to the cortical recording was treated with phenylephrine (10%) and atropine (0.1%), and was equipped with a +2 diopter contact lens. The ipsilateral eye was covered during stimulation. A subcutaneous injection of 0.2 ml 0.1% atropine was administered preoperatively. The retinal landmarks and major retinal blood vessels were projected routinely twice daily onto a tangent screen using a

fiber optic light source (Pettigrew et al. 1979). Area centralis was plotted by reference to the optic disc (14.6 deg medially and 6.5 deg below of the center of optic disc; Bishop et al., 1962).

3.2. Recording

Electrophysiological recording of single units in the AEV and the LM-Sg was carried out extracellularly via tungsten microelectrodes (AM System Inc. USA, 2-4 MOhm). Single-cell discrimination was performed with a spike-separator system (SPS-8701, Australia). Vertical penetrations were performed to reach the LM-Sg between the Horsley-Clarke coordinates anterior 4.5-6.5 and lateral 4-7 in the stereotaxic depths in the interval 10-13 mm. The AEV neurons were recorded between the co-ordinates anterior 11-14 and lateral 12-14 in the stereotaxic depths in the interval 13-19 mm (Reinoso-Suares, 1961). At the end of the experiments, the animals were deeply anaesthetized with pentobarbital and perfused transcardially with paraformaldehyde solution (4%). The brains were removed, cut in coronal sections of 50 μ m and stained with neutral red or for acetylcholine-esterase. Electrolytic lesions marked the locations of successful electrode penetrations. All of the analyzed neurons were located either in the LM-Sg or in the AEV.

3.3. Stimulation and data analysis to compare the internal organisation of the visual receptive fields in the AEV and the LM-Sg

The visual responsivity of the neurons was tested subjectively by the generation of moving visual stimuli with a hand-held lamp. Whenever a single-unit was found to be sensitive to moving visual stimulation, computer-controlled visual noise patterns were used to estimate its visual response properties. For computer-controlled visual stimulation, an 18-inch computer monitor (refresh rate 60 Hz) was placed 57 cm in front of the animal. A stationary visual noise stimulus (grain size: 0.2-1.5°) was presented to the animal in an area of 24° x 32° around the area centralis. The mean luminance of the screen was 17 cd/m². We divided this area into 12 parts each of 8° x 8°. To avoid stationary problems, the stimuli were randomized in position over trials. The randomly selected 8° x 8° portion of the elements comprising the pattern was then moved for 2500 ms at a speed of 10°/s. We

investigated the responses to 8 different moving directions of the visual noise pattern along four axes (0-315° at 45° increments) to find the preferred moving direction of each single neuron. Neuronal activities were then recorded and correlated with the movement of the visual noise pattern in the preferred direction. We tested the internal organisation of the investigated part of the receptive field applying the preferred direction. The data were stored for further analysis as peristimulus time histograms (PSTHs). The prestimulus time (during which a stationary visual noise pattern stimulus was shown) was 500 ms and the peristimulus time (while the visual noise pattern stimulus was moving) was 2500 ms. At least 4 trials were run in each 8° x 8° window. The interstimulus interval was 1 s.

We defined the net firing rate in each 8° x 8° window as the response when a paired t-test demonstrated a significant difference ($p < 0.05$) between the prestimulus and peristimulus firing rates. While the visual receptive field of the AEV and the LM-Sg neurons were consistently larger than the investigated central part of the visual field, we considered a cell to be visually responsive if it was responsive in each 8° x 8° window. The spatial selectivity of each responsive cell was investigated with one-way ANOVA. We defined a neuron as spatially selective if the net firing rate of at least one window was significantly different from the mean of the others. As maximum site, we considered the stimulus location at which the net firing rate was highest. We estimated the distance of the maximum responsive site from the area centralis and the angle of the vector connecting the maximum responsive site and the area centralis. We compared these values between the AEV and the LM-Sg neurons. The comparison was performed either with the t-test, if the values exhibited normal distribution, or with the Kruskal-Wallis test, if the distribution of the values was not normal.

3.4. Stimulation and data analysis to investigate the extent of multisensory receptive fields and the coding of multisensory information in the AEV

For auditory stimulation, we used 12 loudspeakers that were placed at 15° intervals on the 165° perimeter in the interaural plane and delivered white noise (40 dB). The duration of an auditory stimulation was 1 s. The visual stimulus was served by the subsequent lighting of 12 light-emitting-diode (LED) pairs that were placed in the same way on the horizontal plane as the loudspeakers on the 165° perimeter, 30 cm from the eye, in an arc positioned according to the Horsley-Clarke horizontal zero plane. The area

centralis was at 0° on the perimeter. The light emission time of the first LED was 140 ms, and this was followed immediately by emission for 340 ms by the second one. The computer-controlled stimuli were presented in a pseudo-random order, separately or simultaneously (bimodal). The interstimulus interval was 1 s. The number and temporal distribution of action potentials recorded during visual, auditory and bimodal stimulation were stored as peristimulus time histograms (PSTHs) and analyzed off line. The prestimulus time (during we measured the spontaneous activity of the neurons) was 500 ms, and the peristimulus time (during visual, auditory and bimodal stimulus presented) was also 500 ms. Whenever a single unit was found that was visual or auditory-sensitive, at least 10 trials were run in each condition.

The net firing rate was calculated as the difference between the firing rates during the peristimulus and prestimulus time intervals. The net firing rate was defined as a response when a t-test revealed a significant ($p < 0.05$) difference between the two values. The width of the receptive field of a neuron was determined by the locations of stimuli that induced a significant response. As a maximal site we considered those stimulus localizations, at which the net firing rate was the highest. A neuron was regarded as selective to stimulus location when its responses to stimulation in individual locations were significantly different ($p < 0.05$) by one-way analysis of variance (ANOVA). For quantitative characterization of the spatial tuning within a receptive field, we determined the site that induced the largest net response in firing rate and the site that elicited the smallest, but still significant net firing of the cell. We introduced the formula

$$\{(Fr_{\max} - Fr_{\min})/Fr_{\max}\} \times 100 = \text{tuning strength\%}$$

where Fr_{\max} is the net firing rate at the maximal site, and Fr_{\min} is the net firing rate at the smallest, but still significant site. A cross-modal interaction was considered to exist when the difference between the net firing rate of the most effective single modality and the bimodal peristimulus firing rate proved to be significant by ANOVA ($p < 0.05$). The extents of the facilitatory bimodal interactions were determined by the locations of stimuli that induced significant multisensory facilitation. The strength of an interaction was calculated via the formula coined by Meredith and Stein (1986):

$$\{(CM - SM_{\max})/SM_{\max}\} \times 100 = \text{interaction\%}$$

where CM is the mean number of impulses evoked by the bimodal stimulus and SM_{max} is the mean number of impulses evoked by the most effective single-modality stimulus.

3.5. Calculation of the visual response onset latencies

The visual response onset latency was calculated from the neuronal response to stimulate the maximum site of each unit. To measure the onset latency of the responses, we used a software program developed in our laboratory. This was based on a sliding-window technique. The program slid two 300 ms windows along the frequency histogram of the responses. The first window slid through the peristimulus firing rate in one bin steps (5 ms) steps, and selected the 300 ms wide portion that represented the maximum frequency. Then, a second window was slid in one bin steps (5 ms), and after each step the program calculated the significance level between the spike frequency values of the two windows with the t-test. The onset latency of the responses was calculated from the time function of these p values. A curve was fitted to the p values, and the time interval between the start of the stimulation and beginning of the elevation on this curve provides the response latency.

4. Results

4.1 Internal organisation of the visual receptive fields in the AEV and the LM-Sg

The visual receptive field organization and spatial coding abilities of altogether 35 visually responsive single-units in the LM-Sg and 32 in the AEV were analyzed in details. The extent of the visual receptive field was estimated subjectively by listening to the neuronal responses to movements of a light spot generated by a hand-held lamp. Similarly to earlier results, our subjective estimation demonstrated that the visual receptive fields in both the extrageniculate thalamus and the visual associative cortex were extremely large (consistently larger than 6000 deg²): they covered a major part of the contralateral hemifield and extended deep into the ipsilateral one, yielding a field that overlapped almost totally with the visual field of the right eye (Benedek et al., 1997). The receptive fields consistently included the area centralis. No signs of retinotopical organization were observed within either the AEV or the LM-Sg. The visual receptive fields of both the LM-Sg and the AEV neurons were definitely larger than the computer monitor used for visual stimulation. Thus, we could investigate in these experiments the information coding abilities of the AEV and the LM-Sg neurons only in a restricted, though large central part of their visual receptive fields.

The distributions of the preferred directions of the 35 LM-Sg and the 32 AEV units were very similar. Only small proportions of the AEV (3/32) and the LM-Sg neurons (4/35) exhibited optimum responsivity to movement along the horizontal axis (90° and 270° directions). The preferences for the other 6 directions were distributed evenly among the neurons. The data obtained for the optimum directions were used for the further analysis.

Spatial sensitivity towards moving stimulation within the restricted part of the receptive field was estimated by comparing the response intensities by means of one-way ANOVA. This indicated that the majority of the visually responsive neurons in both the LM-Sg (26/35; 73.7%) and the AEV (24/32; 75.0%) were sensitive to the location of the moving visual stimulus (Figs. 2 and 3). The site of maximum responsivity within the visual receptive fields of the AEV and the LM-Sg neurons varied extensively in the neurons recorded. For the most of the units, the visual field did not appear to contain an exclusive site. Some of the units exhibited a preference for a particular stimulus site, while other

units were most responsive to other locations. Maximum responsive sites were found in each quadrant of the visual field (Fig. 4). Thirteen LM-Sg units had a preference in the contralateral upper, 14 in the contralateral lower, 4 in the ipsilateral lower and 4 in the ipsilateral upper quadrant of the investigated central visual field. Similarly twelve AEV cells had a preference in the contralateral upper, 10 in the contralateral lower, 6 in the ipsilateral upper and 4 in the ipsilateral lower quadrant. Our results revealed that the maximum responsive sites of the LM-Sg neurons, similarly to those of the AEV that were distributed throughout the whole of the investigated area. While the receptive fields were much larger than the stimulated central part of the visual field we can not exclude the possibility that some AEV and LM-Sg neurons exhibit maximum responsivity to stimulation sites outside the investigated region. No inhibitory responses were recorded at all.

We estimated the distances of the maximum responsive sites from the area centralis of the AEV and the LM-Sg neurons. The mean distance of the maximum sensitive sites of the AEV neurons from the area centralis was 7.99° (N=32; range: 0-20°; SD: $\pm 4.29^\circ$). The mean distance of the maximum sensitive sites of the LM-Sg neurons from the area centralis was 8.27° (N=35; range: 2-18°; SD: $\pm 3.67^\circ$). Since the distribution of the distances did not satisfy the criterion of normality, we used the Kruskal-Wallis test to compare them. The test demonstrated that there was no significant difference between the distances of the maximum responsive sites from the area centralis of the cortical and that of the thalamic neurons ($p=0.55$). Similar results were obtained as concerns the direction of the line connecting the maximum responsive sites to the area centralis relative to the horizontal meridian. The distributions of the directions for the AEV neurons (mean= 136.5° ; N=32; range: 0-345°; SD: $\pm 118.0^\circ$) and that for the LM-Sg neurons (mean= 146.7° ; N=35; range: 0-350°; SD: $\pm 114.9^\circ$) were very similar. Both displayed a normal distribution. The t-test showed no significant difference between the directions of the sites of maximum sensitivity from the area centralis of the AEV and the LM-Sg neurons ($p=0.87$). These results indicate that the maximum responsive sites of the AEV and the LM-Sg neurons are distributed similarly in the investigated central part of the visual field.

4.2. Extent of visual, auditory and bimodal receptive fields of the AEV neurons

Objective estimation of the visual, auditory and bimodal receptive fields was performed by calculating the significant responses to individual stimulation given at a distance of 15° with the help of the t-test. The width of the receptive field of a neuron was determined by the locations of stimuli that induced a significant response. This procedure obviously underestimates the actual size of the receptive field, but it yields an objective estimate that can be used for further analysis.

The mean extent of the visual receptive fields in the horizontal plane was obtained as 75.8° (N=59; SD: ±28.6°; range: 15-135°; Fig. 5A). Nevertheless, only 4 visual cells revealed significant responses in the whole extent of the 135° field (the visual field of the right eye) studied, in most cases since the peripheral parts of the receptive fields displayed significantly increased responses. The mean extent of the auditory receptive fields in the horizontal plane, as estimated statistically, was found to be 132.5° (N=60; SD: ±46.7°; range: 15-165°; Fig. 5B) in the 165° perimeter examined. Thirty-two auditory cells displayed receptive fields extending to the 165° area studied. The mean bimodal receptive field extent of the bimodal cells in the horizontal plane was 82.1° (N=31; SD: ± 22.2°; range: 30-135°; Fig. 5C). Nine bimodal cells displayed receptive fields extending to the 135° area studied.

4.3. Coding of multisensory information in the AEV

Altogether 219 neurons were recorded in the AEV of the feline brain. Of these, 168 were sensitive to either visual or auditory or combined visual and auditory stimulation. The responses of these 168 neurons were analyzed in detail. Upon comparison of the peristimulus discharge rate with the prestimulus discharge rate, visual sensitivity was found in 95 cells. Ninety-six cells were demonstrated to be auditory-sensitive, while 45 cells proved to be bimodal in the sense that they reacted to a statistically significant extent to both visual and auditory stimulation. Of the 45 bimodal cells, 31 displayed significant responsiveness to separate visual and separate auditory stimulation as well as to simultaneous auditory and visual (bimodal) stimulation. Four cells reacted only to both separately presented visual and auditory modalities, and were insensitive to combined stimulation. Ten cells responded exclusively to simultaneous auditory and visual

stimulation, and were insensitive to separate stimulation with either visual or auditory modalities.

Spatial selectivity towards the site of stimulation within the receptive field was estimated by means of one-way ANOVA. This indicated that 48 of the 95 visual units (50.5%) were selective to the location of the visual stimulus, i.e. at least 2 of their responses to stimulation from different sites of their receptive field differed significantly ($p < 0.05$). Figure 6 shows the responses of a typical panoramic visual neuron that was selective to the stimulus location. The auditory neurons exhibited a much weaker extent of site selectivity. Of the 96 auditory cells, only 26 (27.1%) were selective to the location of the auditory stimulation. Figure 7 shows the responses of a panoramic auditory unit that was found to be selective to the auditory stimulus location. Twenty-five of the 31 bimodal cells (80.6%) that responded to separate visual and separate auditory stimulation and also to simultaneous auditory and visual (bimodal) stimulation were selective to the locations of bimodal stimuli. It is noteworthy that only a much smaller proportion of these 31 neurons were selective to the locations of separate visual (14/31; 45%) and separate auditory (9/31; 29.0%) stimuli. Only 5 neurons were selective to the locations of both unimodal (visual and auditory) and bimodal stimuli. Figure 8 shows the responses of a panoramic bimodal neuron to auditory, visual and bimodal stimulation. This unit elicited vigorous responses to both separate and simultaneously presented auditory and visual stimulation, and was selective to the locations of unimodal (auditory and visual) and bimodal stimuli. Eight of the 10 bimodal cells that responded only to bimodal stimulation and that were insensitive to separate stimulation with either visual or auditory modalities were selective to the bimodal stimulus location.

The sites of maximal responsivity within the large receptive fields to visual, auditory and bimodal stimulation varied extensively in the cells recorded. Sensory stimulation originating from a particular stimulus site produced a maximal response in some cells, while the remainder of the cells had a preference for other sites.

Among the 168 analyzed cells, we found 32 (19.0%) that exhibited a significant cross-modal interaction between simultaneously presented auditory and visual stimuli. A cross-modal response enhancement was observed in 21 of these cells, and a cross-modal depression of the response in 11 cells. It is noteworthy that only 17 of these 32 cells have earlier been defined as bimodal. Fifteen cells with a significant cross-modal interaction originally did not respond to either modality presented alone, but the originally ineffective modality was able to induce either a response enhancement (8 of 15 cells (53.3%)) or a

response depression (7 of 15 cells (46.7%)) when the auditory and visual stimuli were presented simultaneously. We analyzed the receptive field data for the 21 bimodal neurons that exhibited a significant facilitatory cross-modal interaction between visual and auditory stimulation. The mean extent of the facilitatory interaction in these cells was 75.7° (N=21; SD: $\pm 24.6^\circ$; range: 45-135 $^\circ$). We failed to find any site-relatedness of the cross-modal interaction within the perimeter studied. The relationship between the cross-modal facilitation calculated by the formula of Meredith and Stein (1986) and the stimulation site was found by ANOVA to be statistically non significant ($F(9,190)=0.619$, $p=0.78$).

The strength of spatial tuning of the 31 bimodal cells that responded to separate visual and separate auditory stimulation and also to simultaneous auditory and visual (bimodal) stimulation was characterized by calculating the quotient between the maximal response rate and the discharge rate of the minimal significant response in the receptive field (see Methods). This formula yielded a much higher tuning strength in the responses of the bimodal cells to combined auditory and visual stimulation than in response to unimodal auditory or visual stimulation. In these cells, the mean tuning strength of the bimodal stimulation was 60.4% (N=31, SD: $\pm 20.6\%$). The mean tuning strengths of these neurons upon unimodal visual or auditory stimulation were 36.3% (N=31, SD: $\pm 25.1\%$) and 41.1% (N=31, SD: $\pm 22.4\%$), respectively. A t-test demonstrated significant differences between the visual tuning strength and the bimodal tuning strength ($p<0.01$), and between the auditory tuning strength and the bimodal tuning strength ($p<0.01$) of the bimodal cells. The bimodal tuning strength of the bimodal cells was significantly larger than the unimodal auditory or visual tuning strength of the bimodal cells. We calculated the mean distances between the sites that elicited the maximal and the minimal firing rates. These were 48.6° (N=31, SD: $\pm 27.1^\circ$) for the visual response of the bimodal cells, 51.3° (N=31, SD: $\pm 29.9^\circ$) for the auditory response of the bimodal cells, and 46.8° (N=31, SD: $\pm 20.9^\circ$) for the bimodal response of the bimodal cells. There was no significant difference between these distances ($p>0.05$).

4.4. Visual response onset latencies of the AEV and the LM-Sg neurons

We calculated and compared the visual response onset latencies of the 35 investigated LM-Sg and 32 AEV units to assess whether the cortico-thalamic or the thalamo-cortical information processing route has a temporal priority between the LM-Sg

and the AEV (Fig. 9). We calculated the response onset latencies using a PSTH of each unit that was recorded when its maximal responsive site was stimulated. The shortest onset latency in both the LM-Sg and the AEV was 35 ms. Generally, however, the latencies of the responses measured for the AEV units were longer than those for the LM-Sg units. The mean latency of the response of the LM-Sg neurons (calculated at their maximum responsive sites) was 59.4 ms (N=35; range: 35-130 ms; SD: \pm 26.28 ms). The mean latency of the AEV units was 81.7 ms (N=32; range: 35-185 ms; SD: \pm 42.48 ms). The distribution of the AEV and the LM-Sg latencies did not reveal normal distribution, presumably reflecting the fact that there is no homogeneous population of units producing this response. Comparison of the cortical and thalamic latencies by means of the Kruskal-Wallis test revealed that the visual response onset latencies of the investigated LM-Sg neurons were significantly shorter than the visual response onset latencies of the AEV neurons ($p=0.011$).

5. Discussion

5.1. Comparison of the internal organisation of visual receptive fields in the AEV and the LM-Sg

Our results provided evidence that the internal structure of the visual receptive fields of the LM-Sg and the AEV neurons are very similar. Subjective estimation of the extent of visual receptive fields demonstrated that the visual receptive fields in both structures consistently cover the whole visual field of the stimulated eye (Benedek et al., 1997). In this study we investigated the central $24^\circ \times 32^\circ$ part of the receptive fields around the area centralis. The majority of the LM-Sg and the AEV units in our experiments proved to be selective to the stimulus location; they exhibited significantly different responses to stimuli from different spatial locations. These units can provide information via their discharge rate on the site of the visual stimulation. These indicate that they can serve as panoramic localizers at least in the investigate central part of the visual field (Middlebrooks et al., 1994, 1998, 2002). This finding indicated the experiments to investigate the coding of visual and multisensory information within the whole receptive fields that were described in the chapter 4.3. and will be discussed in the chapter 5.3. We found maximal responsive sites in each quadrant. The distribution of the maximal responsive site of the AEV and the LM-Sg neurons were very similar, the maximal sensitive sites of the different single neurons covered the whole investigated central part of the visual filed. This is in agreement with the report from the AEV of Scannell et al. (1986), who found the sites of the most intense responses within the same areas of the receptive fields.

5.2. Objective estimation of the extent of visual and bimodal receptive fields in the AEV

We introduced a quasi-objective, computer-controlled method to investigate the extent of visual and multisensory receptive fields of the AEV neurons. The visual, auditory and the bimodal receptive fields were found to be extremely large. A single visual neuron can carry information from the whole visual field of the right eye, an auditory single-unit carried information from the whole investigated 165° azimuths of the horizontal plane. The

bimodal receptive fields were also extremely large in most cases, the bimodal receptive fields of the bimodal neurons extended to the borders of the visual field of the right eye, although their auditory receptive fields were somewhat larger. The extremely large size of the receptive fields is in contrast with some earlier findings (Olson and Graybiel, 1987; Scannel et al., 1996). In these studies the visual receptive fields were considerably smaller than that described by us. This discrepancy could originate from the different types of anaesthesia used or in the obvious difficulties in drawing these huge receptive fields. Both Olson and Graybiel (1987) and Scannell et al. (1996) concentrated on finding the locations of the most intense areas, while we attempted to find the border between the responsive and absolutely non-responsive areas and sought the locations of the regions of maximum sensitivity.

5.3. Coding of multisensory information in the AEV

Our results furnish new data concerning the multimodal representation of the environment in the feline visual associative cortex. The notion of the existence of a multimodal sensory area over the anterior part of the cat brain is not novel. It was first put forward by Loe and Benevento (1969). Detailed analyses of the visual, somatosensory and auditory properties were performed later (Hicks et al., 1988; Wallace et al., 1992). Our results concerning visual and auditory unimodal cells, together with bimodal cells in the AEV, appear to be entirely in line with these earlier results.

Middlebrooks et al. (1994; 1998; 2002) provided evidence of the panoramic stimulus-localizing ability of neurons in the nontonotopic auditory cortex along the AES. The individual AES neurons can carry information about sound-source locations throughout 360° of azimuth of the horizontal plane and the neuronal responses are stimulus site selective. In this way, one could read the locations of sound sources from the firing patterns of single cortical neurons. Like the auditory ones, the visual neurons in the AES cortex have also extremely large receptive fields (Benedek et al., 1988). In this study we investigated whether the visual and bimodal neurons similarly to the auditory units are panoramic localizers. In contrast with our earlier study (Benedek et al., 2000) we investigated the whole extent of the large visual and bimodal receptive fields. The most noteworthy finding of our results that the single visual and multisensory neurons were selective to stimulus-source location within their large receptive field thus they can serve

as panoramic localizers. The significant selectivity of firing rates for stimulating sites seems to prove that a single neuron is able to distinguish between different stimulus locations. Any single AEV neuron that receives its adequate modality sensory stimulation is able to code the position of a stimulus source over a large perimeter through its firing rate.

The absence of the traditionally topographical code along the AES cortex (Benedek et al., 1988; Middlebrooks et al., 1994) gives the possibility for an alternative mechanism of coding of multisensory information in the AES cortex. A distributed population code was earlier described for sound source location in the AES cortex (Middlebrooks et al., 1998). This distributed population code assumed that the individual neurons are panoramic localizers. The accurate sound-source localization derives from information that is distributed across a large population of such panoramic neurons. Our results demonstrated that the visual and bimodal neurons along the AES cortex similar to the auditory ones are panoramic localizers. Further the different visual and bimodal neurons possess their sites of maximal sensitivity in different parts of their large receptive field. The accurate visual and bimodal stimulus source location can derive from the activity of a large population of such panoramic neurons.

The brain structures that process multisensory information and contain multisensory single cells have the possibility to integrate visual, auditory and somatosensory information. Multisensory integrations, i.e. multisensory response enhancement and depression were earlier described in the intermediate and deep layers of the SC (Meredith and Stein, 1986; Wallace et al., 1998), in the caudate nucleus and in the substantia nigra pars reticulata (Nagy et al., 2006), but we provide here evidence that the single neurons in the AEV have the ability to integrate different sensory modalities. We found both facilitatory and inhibitory interactions, however the majority of the interactions were multisensory response enhancement. Combinations of different modality sensory stimuli would evoke responses that differed substantially from responses to the stimuli individually thus the multisensory information provides more information to the AEV neurons than the individual sensory components. The extent of the bimodal interactions was found to be similar to that of the visual receptive fields. We did not observe any relationship between the strength of the interactions and the stimulation site. Interestingly, some AEV units that exhibited significant multisensory interactions were classified earlier upon the statistical analysis of their responsivity to separate visual and auditory stimuli as unimodal. These units responded in a significant extent to only one modality presented

alone, but the originally significantly not effective modalities were able to induce multisensory interactions. Any AEV unit that show significant cross-modal response enhancement or depression has to be classified as multisensory, thus the analysis of neuronal responsivity to separate visual and auditory stimulation without combination of modalities may strongly underrepresented the number of the multisensory units in the AEV. In order to get comparable results and to exclude the stimulus site related differences on the multisensory integration the sensory stimulations derived from the same positions during the whole study. Thus we were not able to investigate the effect of increasing stimulus disparity on the quality and quantity of the multisensory interactions (Stein et al., 1989; Kadunce et al., 1997; 2001).

The bimodal neurons seem to have the ability to localize the sites of unimodal (visual or auditory) and also bimodal stimuli. When multisensory information tells more to the neurons than the separate visual and auditory stimuli, the bimodal stimulus-source localizing ability of a single multisensory neuron has to be better than its visual and sound-source localizing ability. Accordingly, the large majority of the bimodal AEV neurons were selective to the locations of bimodal stimuli and only a much smaller proportion of these neurons were selective to the locations of separate visual or separate auditory stimuli. Our statistical analysis revealed that the bimodal cells localize more accurately the bimodal stimulus source than the unimodal ones. These results indicate the biological significance of multisensory information processing and cross-modal interactions. Indeed, the merging of multisensory information can help behaving animals to localize the actual source of a stimulus (Stein and Meredith, 1993; Stein and Wallace, 1996).

5.4. The relay function of the LM-Sg

The very high similarity of the receptive fields of the LM-Sg and the AES cortex points to the existence of a very intense exchange of information between the two stages of visual processing. The results of our latency studies provide interesting data on the sequence of volleys of excitation between the cortex and the thalamus. Latency studies are not widely used in the investigation of thalamo-cortical relations, most probably because of the technical limitations in calculating spike latency values amidst considerable spontaneous activity. We found that there was no difference between the shortest latency values of the thalamic and the cortical single-units. Both structures responded to visual

motion with a minimum latency of 35 ms. The mean response latency of the LM-Sg units, however, is significantly shorter than the mean latency of the AEV neurons. These results demonstrate that both the thalamo-cortical and the cortico-thalamic routes are also active between the extrageniculate visual thalamus and the visual associative cortex. The generally shorter latencies in the thalamus might indicate that the visual information flows predominantly from the LM-Sg to the AEV. The fact that there is a temporal priority of the thalamus over the cortex, however, does not prove the superiority of the thalamo-cortical volleys over the cortico-thalamic ones. We can not exclude the possibility either that the information concerning the receptive field properties reaches the LM-Sg (albeit with a delay) through a cortico-thalamic route. Thus the LM-Sg demonstrates strong similarity to other higher order thalamic nuclei, i.e. the lateralis posterior nuclei the medial dorsal nucleus that receive driving from both the cortex and lower centres (Merabet et al., 1998; Casanova et al., 2001; Sommer and Wurtz, 2004). These thalamic nuclei process messages that have already reached the cortex and been processed in at least one cortical area, and at the same time they serve the role of first-order relays receiving signals from the ascending tectal pathways. Since our data suggest that visual information flows bidirectionally between the LM-Sg and the AES cortex, further investigations are necessary to elucidate whether the thalamo-cortical and cortico-thalamic axons are drivers or modulators, and to determine the direction of information flow between the LM-Sg and the AES cortex. Antidromic microstimulation of the AES cortex or the LM-Sg can help reveal direct connections between the responses of the neurons in each area, and neuronal lesions of the LM-Sg or the AES cortex can demonstrate any interdependence of the investigated AES cortex or LM-Sg neuronal activities.

6. Conclusions

Our results demonstrated that the internal organization of the visual receptive fields of the AEV and the LM-Sg neurons are very similar. The visual receptive fields of the AEV and the LM-Sg neurons are also extremely large. The majority of the visual neurons in both structures were selective to the visual stimulus location. The AEV and the LM-Sg neurons can provide information in their discharge rate on the visual stimulus site, thus they can serve as panoramic localizers. The maximal responsive sites of the AEV and the LM-Sg neurons distributed very similar, covered the whole investigated part of the visual field. These observations suggest a distributed population code of visual information in the AEV and similarly in the LM-Sg.

We found that the multisensory AEV neurons are also panoramic localizers and provided evidence on the distributed population code of multisensory information in the AEV. The single multisensory AEV units can integrate multisensory information. The majority of the cross-modal interactions were multisensory response enhancement although we also found multisensory response depression. The bimodal cells localize more accurately the bimodal stimulus source than the unimodal ones. These results indicate the biological significance of multisensory information processing and cross-modal interactions.

The very high similarity of the receptive field organization of the LM-Sg and the AEV points to the existence of a very intense exchange of information between the two stages of visual processing. The LM-Sg takes part in visual information processing through complex thalamo-cortico-thalamic loops. Although the visual information flows predominantly from the LM-Sg to the AEV the comparison of visual response onset latencies between the AEV and the LM-Sg suggest that the cortico-thalamic routes is also active. The LM-Sg represents a thalamic nuclei complex rather similar in function to both the first order and the higher order relay nuclei.

The strong similarities of the physiological responses of the LM-Sg and the AEV, together with the fact that the SC provides their common ascending source of information suggest the particular role of the tecto-LM-Sg-AEV system in multisensory information processing and sensory-motor integration.

7. Summary

Electrophysiological recording of single units in the AEV and the LM-Sg was carried out extracellularly via tungsten microelectrodes in halothane-anesthetized, immobilized, artificially respired cats. Neuronal activities were recorded and correlated with the visual, auditory and multisensory stimulation and stored for further analysis as peristimulus time histograms (PSTHs). The net firing rate was calculated as the difference between the firing rates during the prestimulus and peristimulus intervals. The net firing rate was defined as a response when a t-test revealed a significant ($p < 0.05$) difference between the two values. Vertical penetrations were performed to reach the LM-Sg between the Horsley-Clarke coordinates anterior 4.5-6.5 and lateral 4-7 in the stereotaxic depths in the interval between 10-13 mm. The AEV neurons were recorded between the co-ordinates anterior 11-14 and lateral 12-14 in the stereotaxic depths in the interval between 13-19 mm.

The visual receptive field organisation and spatial coding abilities of altogether 35 visually responsive single-units in the LM-Sg and 32 in the AEV was analyzed in the central $24^\circ \times 32^\circ$ part of the visual field. The visual receptive fields in both the AEV and the LM-Sg were extremely large (consistently larger than 6000 deg^2): they covered almost totally the visual field of the investigated eye thus we mapped only a restricted, central part of the receptive fields. We observed no signs of retinotopical organization within either the AEV or the LM-Sg. The majority of the visually responsive neurons in both the LM-Sg (26/35) and the AEV (24/32) was sensitive to the location of the moving visual stimulus, i.e. at least 2 of their responses to stimulation from different sites of their receptive field differed significantly ($p < 0.05$). No inhibitory responses were recorded at all. The site of maximum responsivity within the visual receptive fields of the AEV and the LM-Sg neurons varied extensively in the neurons recorded. Maximum responsive sites were found in each quadrant of the visual field. The maximum responsive sites of the AEV and the LM-Sg neurons were distributed similarly. These findings suggest a distributed population code of visual information in the AEV and similarly in the LM-Sg.

We checked the spatial coding of multisensory information in the AEV. We analyzed the information coding ability within the whole, extremely large receptive fields of 95 visual-sensitive, 96 auditory-sensitive, and 45 multisensory neurons that reacted to both visual and auditory stimulation. This indicated that the majority of the visual units were selective to the location of the visual stimulus. The auditory neurons exhibited a

much weaker extent of site selectivity. Only one quarter of the auditory units was selective to the location of the auditory stimulation. The large majority of the bimodal cells were selective to the locations of bimodal stimuli. It is noteworthy that only a much smaller proportion of these multisensory neurons were selective to the locations of separate visual and separate auditory stimuli. The sites of maximal responsivity within the large receptive fields to visual, auditory and bimodal stimulation varied extensively in the cells recorded. Sensory stimulation originating from a particular stimulus site produced a maximal response in some cells, while the remainder of the cells had a preference for other sites. Our results suggest a distributed population code of multisensory spatial information based on multisensory panoramic localizer neurons in the AEV.

A substantial proportion of the multisensory AEV units exhibited a significant cross-modal interaction between simultaneously presented auditory and visual stimuli. It means that the AEV units have the ability to integrate the simultaneously presented single sensory components and process them as complex multisensory information. The majority of the interactions were cross-modal response enhancement, while we also described cross-modal depression. We found no site-relatedness of the magnitude of cross-modal interactions within the perimeter studied. Fifteen cells with a significant cross-modal interaction originally did not respond in a significant extent to either modality presented alone, but the originally ineffective modality was able to induce either a response enhancement or a response depression when the auditory and visual stimuli were presented simultaneously. These units have to be considered also as multisensory, thus the investigation of auditory and visual modalities alone without combination of modalities might strongly underrepresent in earlier studies the number of multisensory AEV units.

Our statistical analysis revealed that the ability of bimodal cells to localize a bimodal stimulus source is superior to any kind of unimodal (visual or auditory) localization function. These results indicate the biological significance of bimodal information processing and cross-modal interactions. Indeed, the merging of bimodal information can help behaving animals to localize the actual source of a stimulus

The very high similarity of the receptive field organization of the LM-Sg and the AEV neurons points to the existence of a very intense exchange of information between the two stages of visual processing. The LM-Sg takes part in visual information processing through complex thalamo-cortico-thalamic loops. We calculated and compared the visual response onset latencies of the LM-Sg and the AEV units to assess whether the cortico-thalamic or the thalamo-cortical information processing route has a temporal priority

between the LM-Sg and the AEV. Although the shortest onset latency in both the LM-Sg and the AEV was similarly 35 ms, generally the mean onset latency of the response of the LM-Sg neurons (calculated at their maximum responsive sites) was significantly shorter than those for the AEV units. These results suggest that both the thalamo-cortical and the cortico-thalamic routes are active between the extrageniculate visual thalamus and the visual associative cortex. The LM-Sg represent a thalamic nucleus very similar in function to both the first order and higher order thalamic relays although the generally shorter latencies in the LM-Sg might indicate its primary function to relay the tectal visual information to the AES cortex.

Our results presented above add new data concerning the visual and multimodal representation of the environment in the mammalian brain. The strong similarities of the visual receptive field organization and the physiological responses of the LM-Sg and the AEV, together with the fact that the SC provides their common ascending source of information, suggest their common function in multisensory information processing and sensory-motor integration.

8. Acknowledgments

I greatly appreciate the helpful and instructive guidance of my professor and supervisor Dr. György Benedek. I wish to express my deepest thanks to Dr. Attila Nagy for his generously help and support during my scientific work. I express my most sincere gratitude to Gabriella Dósai for her valuable technical assistance and for the preparation of high-quality figures for my dissertation. Many thanks are due to Péter Liszli for his expert help in solving hardware and software problems. I would like to acknowledge the help of Dr. Antal Berényi, Ágnes Farkas, Dr. Zita Márkus, Andrea Pető and Dr. Alíz Roxine in the data collection. I express my gratitude to Dr. Zoltán Chadaide, Károly Köteles, Zsuzsanna Paróczy, Dr. Gyula Sáy and Dr. Tamás Tompa my direct colleagues in the Visual Laboratory for their help and friendship. I would like to express my deepest thanks to all colleagues in the Department of Physiology for their support. It was good to work with them in that department.

My deepest thanks are due to my family for their continuous love and help in my life.

Our experiments were supported by OTKA/Hungary grant 29817, OTKA/Hungary grant T42610 and FKFP/Hungary grant 0455/2000.

9. References

- Benedek G, Hicks TP (1988) The visual insular cortex of the cat: organization, properties and modality specificity. *Prog Brain Res* 75:271-278
- Benedek G, Jang EK, Hicks TP (1986) Physiological properties of visually responsive neurones in the insular cortex of the cat. *Neurosci Lett* 64:269-274
- Benedek G, Mucke L, Norita M, Albowitz B, Creutzfeldt OD (1988) Anterior ectosylvian visual area (AEV) of the cat: physiological properties. *Prog Brain Res* 75:245-255
- Benedek G, Sztriha L, Kovács G (2000) Coding of spatial co-ordinates on neurones of the feline visual association cortex. *Neuroreport* 11:1-4
- Benedek G, Perényi J, Kovács G, Fischer-Szatmári L, Katoh YY (1997) Visual, somatosensory, auditory and nociceptive modality properties in the feline supragenulate nucleus. *Neuroscience* 78:179-189
- Benedek G, Fischer-Szatmári L, Kovács G, Perényi J, Katoh YY (1996) Visual, somatosensory and auditory modality properties along the feline supragenulate-anterior ectosylvian sulcus/insular pathway. *Prog Brain Res* 112:325-334
- Bialek W, Rieke F, de Ruyter van Steveninck RR, Warland D (1991) Reading a neural code. *Science* 252:1854-1857
- Bishop PO, Kozak W, Vakkur GJ (1962) Some quantitative aspects of the cat's eye: axis and plane of reference, visual field coordinates and optics. *J Physiol* 163:466–502
- Brugge JF, Reale RA, Jenison RL, Shupp J (2001) Auditory cortical spatial receptive field. *Audiol Neurootol* 6:173-177

Casanova C, Merabet L, Desautels A, Minville K (2001) Higher-order motion processing in the pulvinar. *Prog Brain Res* 134:71-82.

Comoli E, Coizet V, Boyes J, Bolam JP, Canteras NS, Quirk RH, Overton PG, Redgrave P (2003) A direct projection from superior colliculus to substantia nigra for detecting salient visual events. *Nat Neurosci* 6:974-980

Furukawa S, Xu L, Middlebrooks JC (2000) Coding of sound-source location by ensembles of cortical neurones. *J Neurosci* 20:1216-1228

Goldring JE, Dorris MC, Corneil BD, Ballantyne PA, Munoz DP (1996) Combined eye-head gaze shifts to visual and auditory targets in humans. *Exp Brain Res* 111:68-78

Guillery RW, Feig SL, Van Lieshout DP (2001) Connections of higher order visual relays in the thalamus: a study of corticothalamic pathways in cats. *J Comp Neurol* 438:66-85

Guillery RW, Sherman SM (2002) Thalamic relay functions and their role in corticocortical communication: generalizations from the visual system. *Neuron* 33:163-175

Hardy H, Heimer L, Switzer R, Watkins D (1976) Simultaneous demonstration of horseradish peroxidase and acetylcholinesterase. *Neurosci Lett* 3:1-15

Harting JK, Updyke BV, Van Lieshout DP (1992) Corticotectal projections in the cat: anterograde transport studies of twenty-five cortical areas. *J Comp Neurol* 324:379-414

Harting JK, Updyke BV, Van Lieshout DP (2001a) Striatal projections from the cat visual thalamus. *Eur J Neurosci* 14:893-896

Harting JK, Updyke BV, Van Lieshout DP (2001b) The visual-oculomotor striatum of the cat: functional relationship to the superior colliculus. *Exp Brain Res* 136:138-142

Hicks TP, Benedek G, Thurlow GA (1988a) Modality specificity of neuronal responses within the cat's insula. *J Neurophysiol* 60:422-437

Hicks TP, Benedek G, Thurlow GA (1988b) Organization and properties of neurons in a visual area within the insular cortex of the cat. *J Neurophysiol* 60:397-421

Hicks TP, Stark CA, Fletcher WA (1986) Origins of afferents to visual supragenulate nucleus of the cat. *J Comp Neurol* 246:544-554

Hoshino K, Katoh YY, Bai W, Kaiya T, Norita M (2000) Distribution of terminals from pedunculo-pontine tegmental nucleus and synaptic organization in lateralis medialis-supragenulate nucleus of cat's thalamus: anterograde tracing, immunohistochemical studies and quantitative analysis. *Visual Neurosci* 17:893-904

Hoshino K, Nagy A, Eördegh G, Benedek G, Norita M (2004) Two types of neuron are found within the PPT, a small percentage of which project to both the LM-SG and SC. *Exp Brain Res* 155:421-426

Hubel DH, Wiesel TN (1962) Receptive fields, binocular interaction and functional architecture in the cat's visual cortex. *J Physiol* 160:106-154

Hubel DH, Wiesel TN (1961) Integrative action in the cat's lateral geniculate body. *J Physiol* 155:385-398

Jay MF, Sparks DL (1984) Auditory receptive fields in primate superior colliculus shift with changes in eye position. *Nature* 309:345-347

Jiang H, Lepore F, Ptito M, Guillemot J-P (1994) Sensory modality distribution in the anterior cingulate cortex (AEC) of cats. *Exp Brain Res* 97:404-414

Jiang H, Stein BE, McHaffie JG (2003) Opposing basal ganglia processes shape midbrain visuomotor activity bilaterally. *Nature* 424:982-986

Kadunce DC, Vaughan JW, Wallace MT, Benedek G, Stein BE (1997) Mechanisms of within- and cross-modality suppression in the superior colliculus. *J Neurophysiol* 78:2834-2847

Kadunce DC, Vaughan JW, Wallace MT, Stein BE (2001) The influence of visual and auditory receptive field organization on multisensory integration in the superior colliculus. *Exp Brain Res* 139:303-310

Katoh YY, Arai R, Benedek G (2000) Bifurcating projections from the cerebellar fastigial neurons to the thalamic suprageniculate nucleus and to the superior colliculus. *Brain Res* 864:308-311

Katoh YY, Benedek G, Deura S (1995) Bilateral projections from the superior colliculus to the suprageniculate nucleus in the cat: a WGA-HRP/double fluorescent tracing study. *Brain Res* 669:298-302

Katoh YY, Benedek G (1995) Organization of the colliculo-suprageniculate pathway in the cat: a wheat germ agglutinin-horseradish peroxidase study. *J Comp Neurol* 352:381-397

Katoh YY, Benedek G (2003) Cerebellar fastigial neurons send bifurcating axons to both the left and right superior colliculus in cats. *Brain Res* 970:246-249

King AJ, Hutchings ME (1987) Spatial response properties of acoustically responsive neurons in the superior colliculus of the ferret: a map of auditory space. *J Neurophysiol* 57:596-624

Knudsen EI (1982) Auditory and visual maps of space in the optic tectum of the owl. *J Neurosci* 2:1177-1194

Lewis JE (1999) Sensory processing and the network mechanisms for reading neuronal population codes. *J Comp Physiol* 185:373-378

Lee C, Rohrer WH, Sparks DL (1988) Population coding of saccadic eye movements by neurons in the superior colliculus. *Nature* 332:357-360

Loe PR, Benevento LA (1969) Auditory-visual interaction in single units in the orbito-insular cortex of the cat. *Electroencephalogr Clin Neurophysiol* 26:395-398

Merabet L, Desautels A, Minville K, Casanova C (1998) Motion integration in a thalamic visual nucleus. *Nature* 396:265-268

Meredith MA, Stein BE (1986) Visual, auditory and somatosensory convergence on cells in superior colliculus results in multisensory integration. *J Neurophysiol* 56:640-662

Meredith MA, Wallace MT, Stein BE (1992) Visual, auditory and somatosensory convergence in output neurons of the cat superior colliculus: multisensory properties of the tecto-reticulo-spinal projection. *Exp Brain Res* 88:181-186

Miceli D, Reperant J, Ptito M (1985) Intracortical connections of the anterior ectosylvian and lateral suprasylvian visual areas in the cat. *Brain Res* 347:291-298

Middlebrooks JC, Clock AE, Xu L, Green DM (1994) A panoramic code for sound location by cortical neurons. *Science* 264:842-844

Middlebrooks JC, Xu L, Eddins AC, Green DM (1998) Codes for sound-source location in nontopographic auditory cortex. *J Neurophysiol* 80:863-882

Middlebrooks JC, Xu L, Furukawa S, Macpherson EA (2002) Cortical neurones that localize sounds. *Neuroscientist* 8:73-83

Middlebrooks JC, Knudsen EI (1984) A neural code for auditory space in the cat's superior colliculus. *J Neurosci* 4:2621-2634

Mucke L, Norita M, Benedek G, Creutzfeldt OD (1982) Physiologic and anatomic investigation of a visual cortical area situated in the ventral bank of the anterior ectosylvian sulcus of the cat. *Exp Brain Res* 46:1-11

Nagy A, Eördegh G, Norita M, Benedek G (2003) Visual receptive field properties of neurons in the feline caudate nucleus. *Eur J Neurosci* 18:449-452

Nagy A, Eördegh G, Norita M, Benedek G (2005a) Visual receptive field properties of excitatory neurons in the substantia nigra. *Neuroscience* 130:513-518

Nagy A, Paróczy Z, Norita M, Benedek G (2005b) Multisensory responses and receptive field properties of neurons in the substantia nigra and in the caudate nucleus. *Eur J Neurosci* 22:419-424

Nagy A, Eördegh G, Paróczy Z, Márkus Z, Benedek G (2006) Multisensory integration in the basal ganglia. *Eur J Neurosci* 24:917-924

Nalbach HO, Thier P, Varju D (1993) Binocular interaction in the optokinetic system of the crab *Carcinus maenas* (L.): optokinetic gain modified by bilateral image flow. *Vis Neurosci* 10:873-885

Norita M, Hicks TP, Benedek G, Katoh YY (1991) Organization of cortical and subcortical projections to the feline insular visual area, IVA. *J Hirnforsch* 32:119-134

Norita M, Mucke L, Benedek G, Albowitz B, Katoh YY, Creutzfeldt OD (1986) Connections of the anterior ectosylvian visual area (AEV). *Exp Brain Res* 62:225-240

Olson CR, Graybiel AM (1987) Ectosylvian visual area of the cat: location, retinotopic organization, and connections. *J Comp Neurol* 261:277-294

Olson CR, Graybiel AM (1983) An outlying visual area in the cerebral cortex of the cat. *Prog Brain Res* 58:239-245

Palmer AR, King AJ (1982) The representation of auditory space in the mammalian superior colliculus. *Nature* 299:248-249

Pettigrew JD, Cooper ML, Blasdel GG (1979) Improved use of tapetal reflection for eye-position monitoring. *Invest Ophthalmol Vis Sci* 18:490-495

Reinoso-Suarez F, Roda JM (1985) Topographical organization of the cortical afferent connections to the cortex of the anterior ectosylvian sulcus in the cat. *Exp Brain Res* 59:313-324

Reinoso-Suarez F (1961) Topographischer Hirnatlas der Katze für experimental-physiologische Untersuchungen. Darmstadt, Meck AG

Rosenquist AC (1985) Cerebral Cortex Volume 3 Visual Cortex. Peters A, Jones EG editors Connections of visual Cortical Areas in the Cat. New York, Plenum Press 81-117

Sanderson KJ (1971) The projection of the visual field to the lateral geniculate and medial interlaminar nuclei in the cat. *J Comp Neurol* 143:101-108

Scannell JW, Sengpiel F, Tovee MJ, Benson PJ, Blakemore C, Young MP (1996) Visual motion processing in the anterior ectosylvian sulcus of the cat. *J Neurophysiol* 76:895-907

Sherman SM, Guillery RW (1998) On the actions that one nerve cell can have on another: distinguishing "drivers" from "modulators". *Proc Natl Acad Sci* 95:7121-7126

Sherman SM, Guillery RW (2002) The role of the thalamus in the flow of information to the cortex. *Philos Trans R Soc Lond B Biol Sci* 357:1695-1708

Sommer MA, Wurtz RH (2004) What the brain stem tells the frontal cortex. I. Oculomotor signals sent from superior colliculus to frontal eye field via mediodorsal thalamus. *J Neurophysiol* 91:1381-1402

Stein BE, Meredith MA, Huneycutt WS, McDade L (1989) Behavioral indices of multisensory integration: orientation to visual cues is affected by auditory stimuli. *J Cogn Neurosci* 1:12-24

Stein BE, Meredith MA (1993) *The Merging of the Senses*. Cambridge, MIT Press

Stein BE, Wallace MT (1996) Comparisons of cross-modality integration in midbrain and cortex. *Prog Brain Res* 112:289-299

Taylor TL, Klein RM, Munoz DP (1999) Saccadic performance as a function of the presence and disappearance of auditory and visual fixation stimuli. *J Cogn Neurosci* 11:206-213

Tusa RJ, Palmer LA, Rosenquist AC (1978) The retinotopic organization of area 17 (striate cortex) in the cat. *J Comp Neurol* 177:213-235

Updyke BV (1981) Projections from visual areas of the middle suprasylvian sulcus onto the lateral posterior complex and adjacent thalamic nuclei in cat. *J Comp Neurol* 201:477-506

Villeneuve MY, Casanova C (2003) On the use of isoflurane versus halothane in the study of visual response properties of single cells in the primary visual cortex. *J Neurosci Meth* 129: 19-31

Wallace MT, Meredith MA, Stein BE (1992) Integration of multiple sensory modalities in cat cortex. *Exp Brain Res* 91:484-488

Wallace MT, Meredith MA, Stein BE (1998) Multisensory integration in the superior colliculus of the alert cat. *J Neurophysiol* 80:1006-1010

Wang C, Dreher B, Assaad N, Ptito M, Burke W (1998) Excitatory convergence of Y and non-Y channels onto single neurons in the anterior ectosylvian visual area of the cat. *Eur J Neurosci* 10:2945-2956

Wang C, Waleszczyk WJ, Benedek G, Burke W, Dreher B (2001) Convergence of Y and non-Y channels onto single neurons in the superior colliculi of the cat. *Neuroreport* 12:2927-2933

10. Figures and figure captions

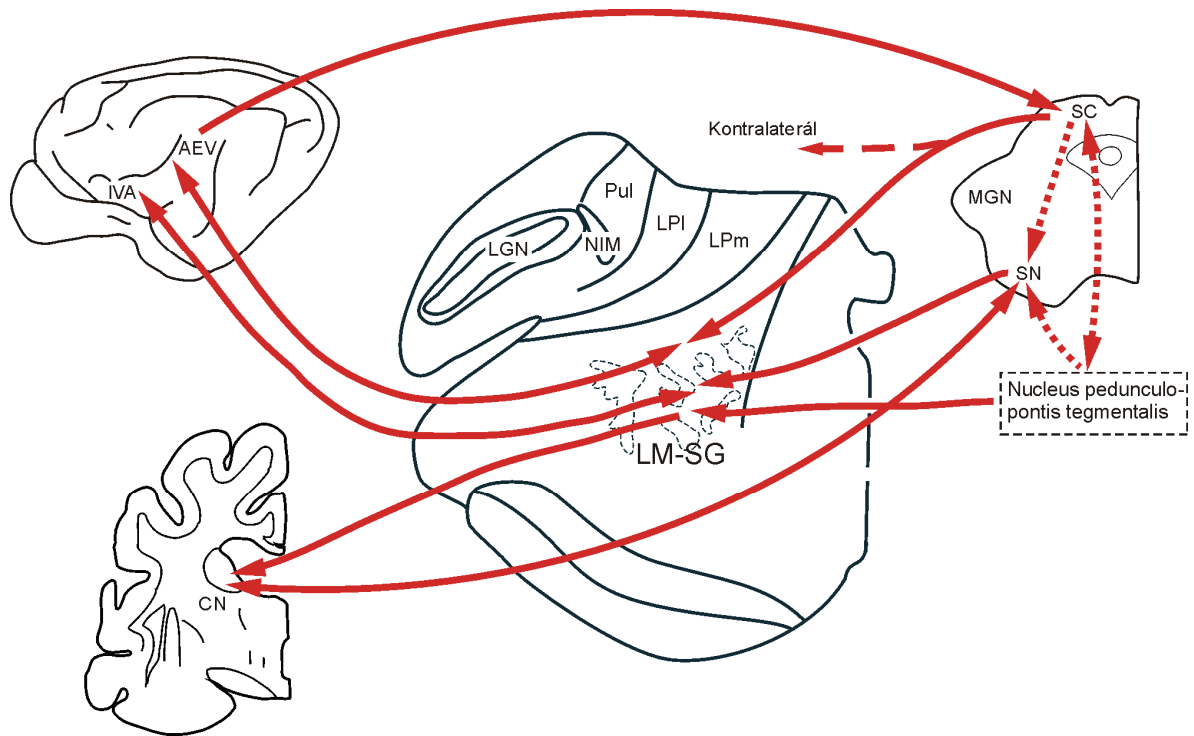


Figure 1

Connections within the tectal extrageniculate visual system in the feline brain. Abbreviations: AEV: anterior ectosylvian visual area, CN: caudate nucleus, IVA: insular visual area, LGN: lateral geniculate nucleus, MGN: medial geniculate nucleus, LM-SG: lateralis medialis-suprageniculate nucleus, LPm: medial division of lateral posterior nucleus, LPI: lateral division of lateral posterior nucleus, Pul: pulvinar, SC: superior colliculus, SN: substantia nigra.

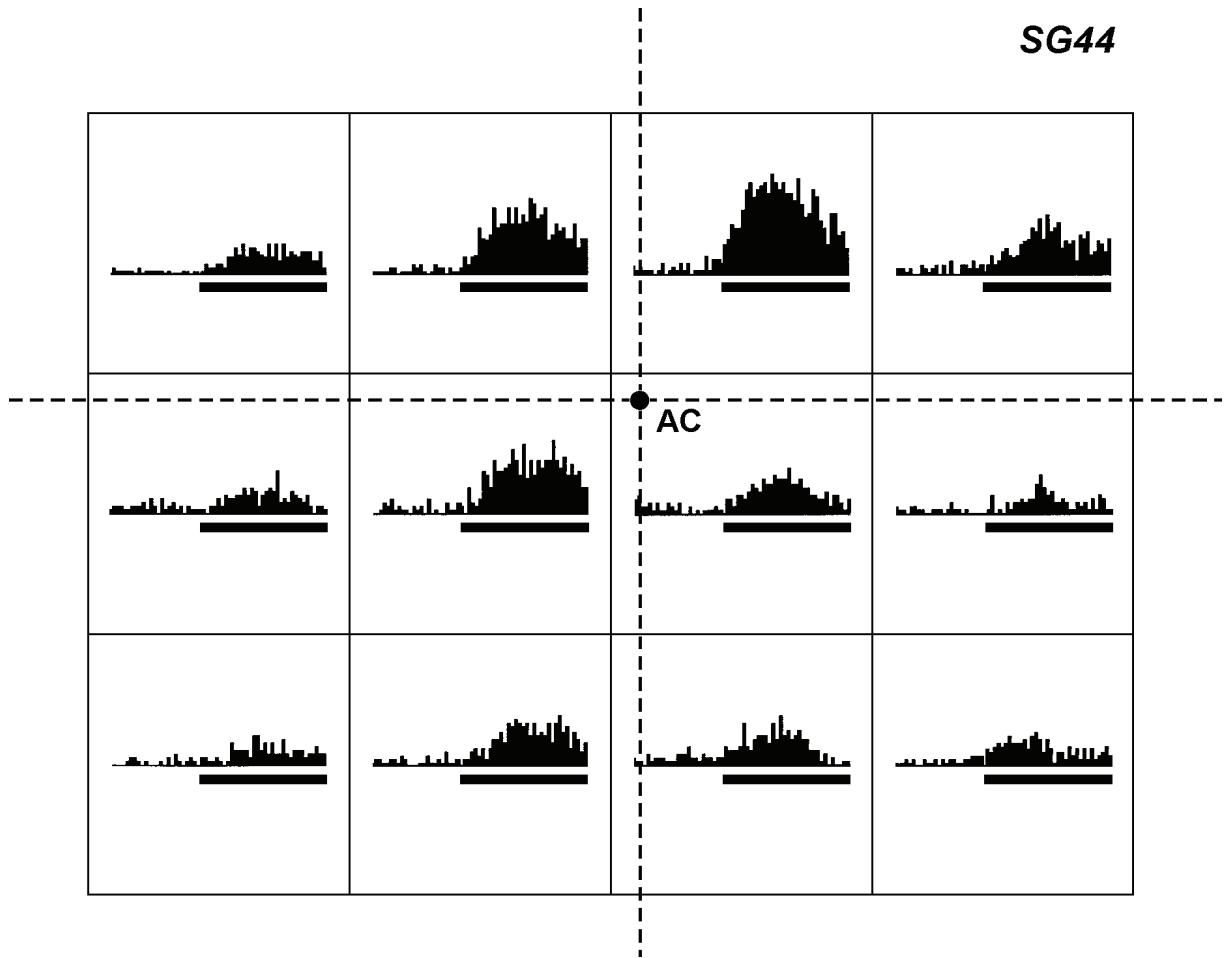


Figure 2

Receptive field organization of a panoramic LM-Sg neuron. Peristimulus histograms are presented that were recorded during the motion of visual noise in the respective part of the visual field. Each window represents a $8^\circ \times 8^\circ$ portion of the receptive field. In each window, the abscissa indicates time. The ordinate denotes number of action potential/binwidth values (binwidth = 62 ms). The thick black line indicates the motion of the visual noise for 2500 ms.

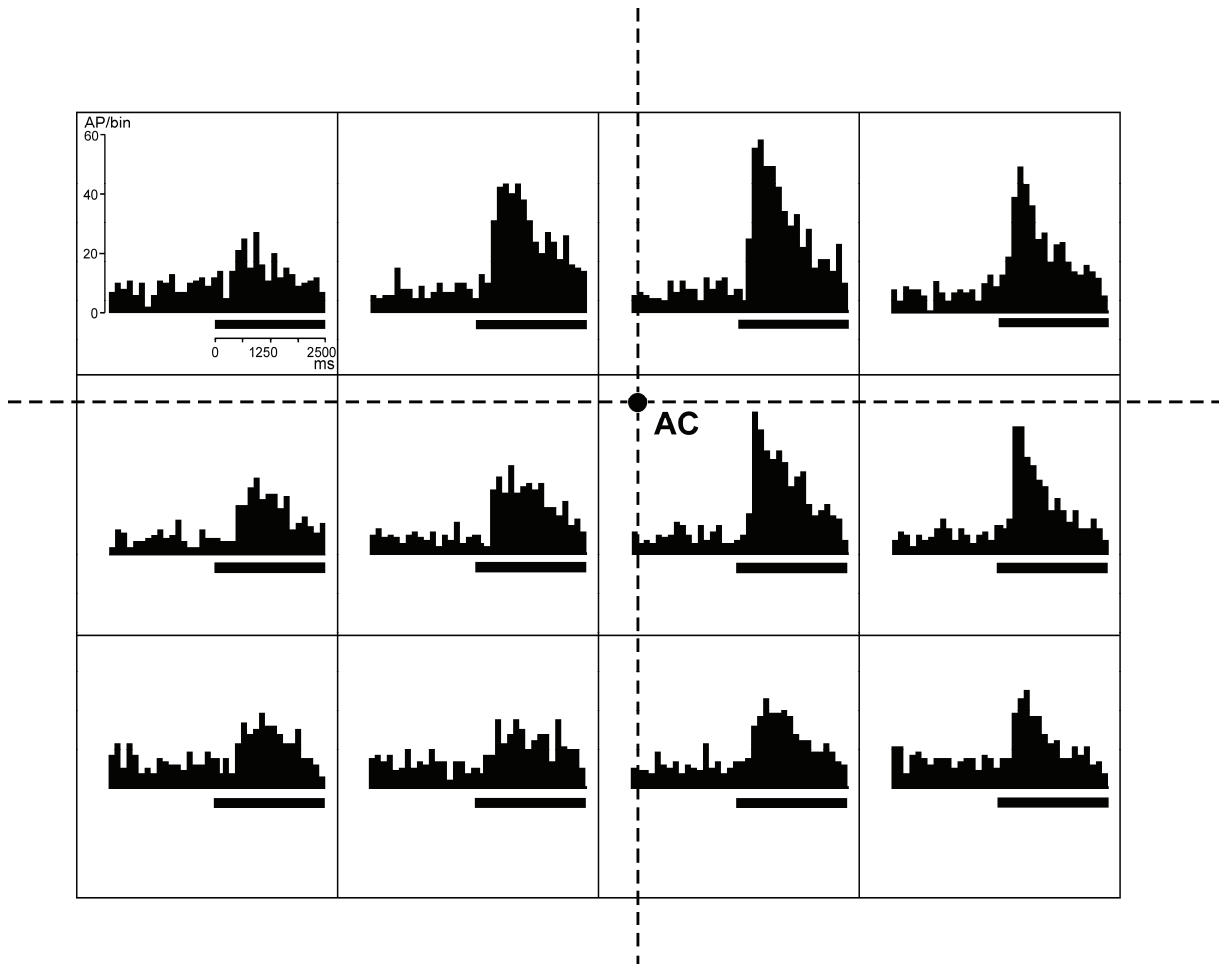


Figure 3

Receptive field organization of a panoramic AEV neuron. Peristimulus histograms were recorded during the motion of visual noise in the respective part of the visual field. Each window represents a $8^\circ \times 8^\circ$ portion of the receptive field. In each window, the abscissa indicates time. The ordinate denotes number of action potential/binwidth values (binwidth = 124 ms). The thick black line indicates the motion of the visual noise for 2500 ms.

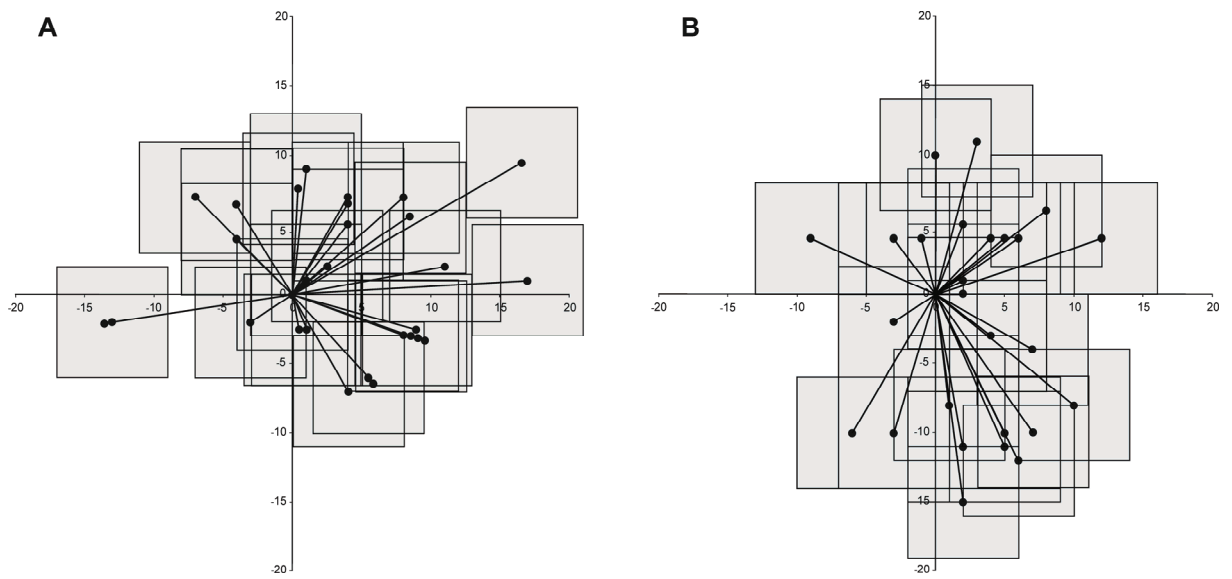


Figure 4

Position of the site of maximum responsivity in the receptive fields of 32 AEV (A) and 35 LM-Sg single-units (B) determined by the highest firing rate in the respective window. Every single-unit is represented by an $8^\circ \times 8^\circ$ grey window representing the motion of the visual noise and a vector line between the area centralis and the centre of the “window” from where the highest activity was elicited. Vertical and horizontal meridians are presented as thick lines, with scaling given in degrees.

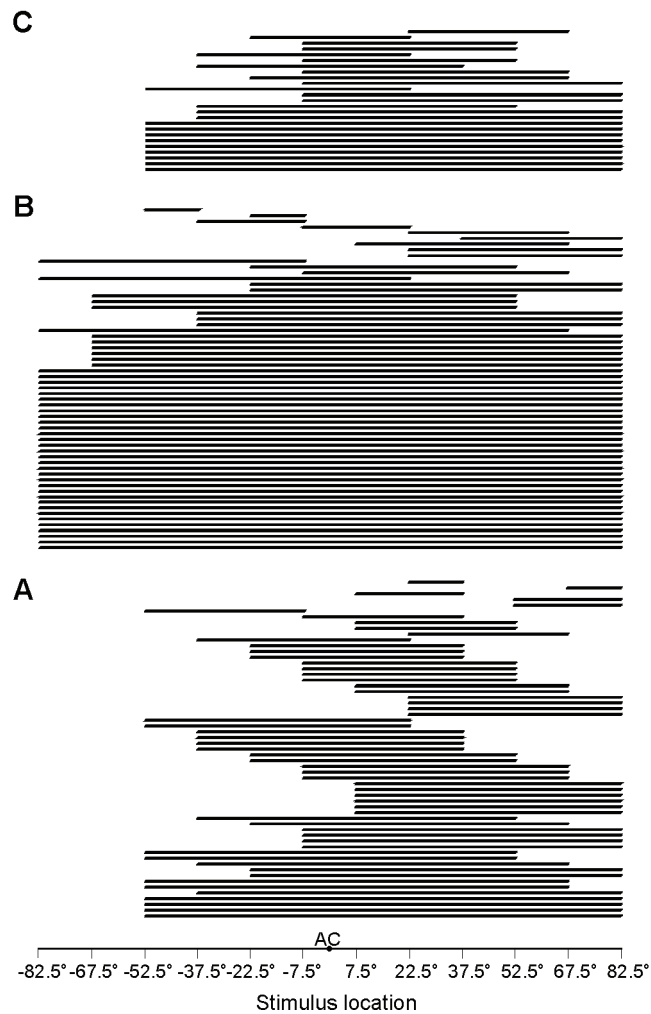


Figure 5

The extents of 59 visual (A), 60 auditory (B) and 31 bimodal (both auditory and visual) receptive fields (C) of AEV neurons estimated by our objective, statistical method. The numbers in degrees indicate the sites of the stimuli related to the area centralis in the horizontal plane. Horizontal lines reveal statistically significant increases in the firing rate as responses to stimulation in the corresponding part of the receptive field. Abbreviation: AC = area centralis.

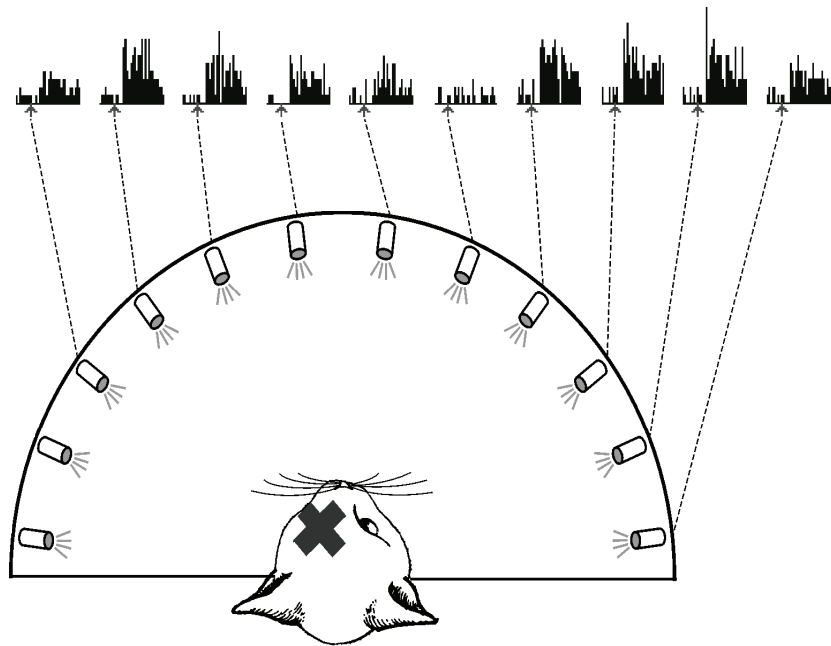


Figure 6

Schematic drawing of the visual stimulating set-up (bottom) and PSTHs of a panoramic AEV neuron (top). The arrows under the PSTHs indicate the start of the visual stimulus presentation. On the PSTHs to the left of the arrows, the spontaneous activity of the recorded neuron can be seen. The schematic bulbs represent the positions of the LED diodes. The neuron elicited vigorous and differing responses to the different stimulus locations tested. Broken lines point to the corresponding histograms.

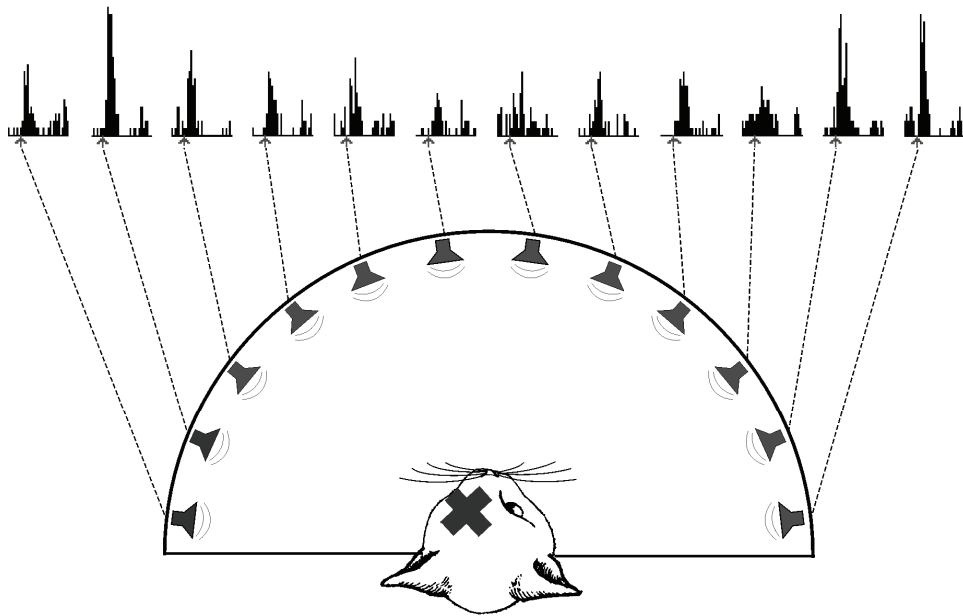


Figure 7

Schematic drawing of the auditory stimulating set-up (bottom) and PSTHs of a panoramic AES cortex neuron (top). The arrows under the PSTHs indicate the start of the auditory stimulus presentation. On the PSTHs to the left of the arrows, the spontaneous activity of the recorded neuron can be seen. The schematic bulbs represent the positions of the loudspeakers. The neuron elicited vigorous and differing responses to the different stimulus locations tested. Broken lines point to the corresponding histograms.

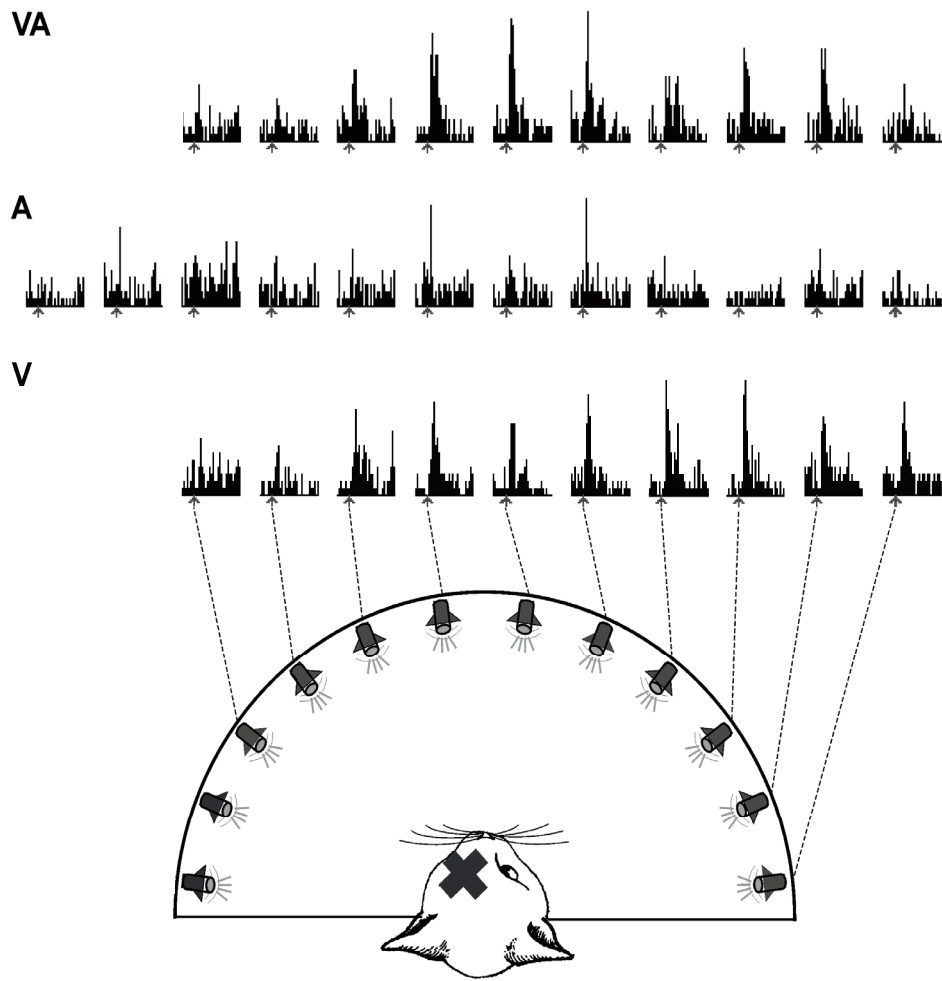


Figure 8

Schematic drawing of the bimodal stimulating set-up (bottom) and peristimulus time histograms of the discharge of one panoramic bimodal AEV neuron responding to visual (V), auditory (A) and simultaneous auditory and visual (AV) stimulation (top). The arrows under the PSTHs indicate the start of the visual, auditory and bimodal stimulus presentation. On the PSTHs to the left of the arrow, the spontaneous activity of the recorded neuron can be seen. This unit responded vigorously to visual, auditory and bimodal stimulation, and was selective to the locations of the visual, auditory and bimodal stimuli. Schematic bulbs and loudspeakers represent the positions of acoustic and visual stimuli, respectively. Broken lines point to the corresponding histograms.

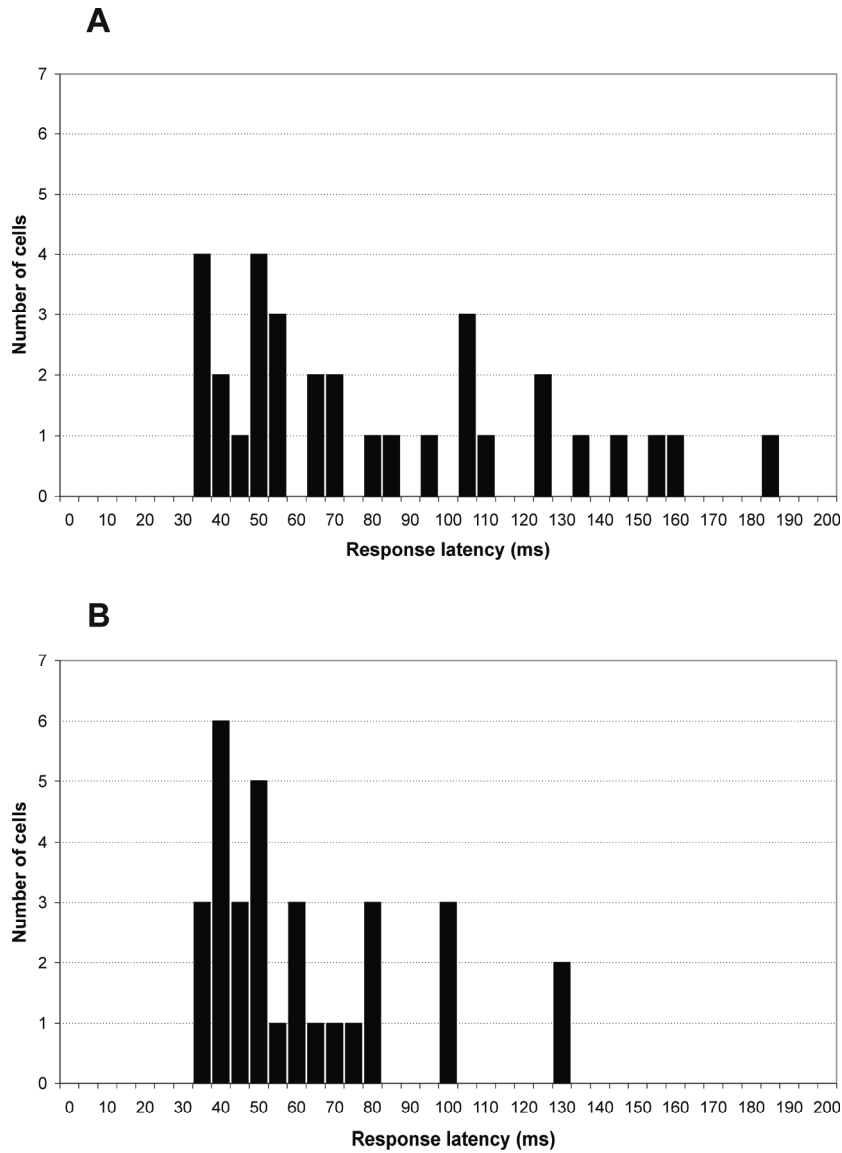


Figure 9

Frequency distributions of AEV (A) and LM-Sg (B) neurons according to their response latency to a visual noise moving in their receptive fields. The abscissa shows the latency of the single-unit activity response in ms. The ordinate indicates the numbers of units with the respective latency values.